Observation of Temporal Behavior of an Atomic Wave Packet Localized in an Optical Potential

M. Kozuma,[1] K. Nakagawa,[2] W. Jhe,[3] and M. Ohtsu[1,4]

[1]*Interdisciplinary Graduate School of Science and Engineering, Tokyo Institute of Technology, 4259, Nagatsuta-cho, Midori-ku, Yokohama 226, Japan*

[2]*Tokyo Institute of Polytechnics, 1583, Iiyama-cho, Atugi 243-02, Japan*

[3]*Department of Physics, Seoul National University, Seoul 151-742, Korea*

[4]*Kanagawa Academy of Science and Technology, KSP East 408, 3-2-1 Sakado, Takatsu-ku, Kawasaki 213, Japan*

(Received 8 November 1995)

We have investigated the dynamic temporal behavior of atomic motion in a periodic optical potential by detecting a recoil-induced resonance signal. In the slowly moving optical potential, damped oscillations are observed in the transient signal and the oscillation frequency is found to be independent of the moving speed of the potential. By using a Monte Carlo wave-function method, the signal can be attributed to the oscillatory motion of atomic wave packet localized in the potential, where the oscillation frequency corresponds to the energy separation between vibrational levels.

PACS numbers: 32.80.Lg, 32.80.Pj

There has been much interest in the quantized motion of cold atoms inside a periodic optical potential. The discrete vibrational energy spectrum therein has been spectroscopically observed by using a stimulated Raman technique [1] and a heterodyne technique [2,3]. However, in spite of the natural expectation, the dynamic behavior of the atomic motion localized in the optical potential, which can be understood as a result of quantum interference between the stationary discrete vibrational eigenstates, has not been observed yet. Observation of such a dynamics can provide one the information on an atomic coherence time.

Recently, atomic motion traversing a periodic optical potential was observed [4] by detecting the transient response of the recoil-induced resonance signal [5,6] when two probes were introduced into cold atoms. In that work, localized atoms were first produced in a stationary periodic optical potential produced by the interference between two probe beams having the same frequencies. With the frequency difference shifted to some large value, the atoms were then made to acquire an initial kinetic energy, in the frame of the moving optical potential, much larger than the potential depth itself. Therefore, they could transverse many such potentials, which was manifested as a decaying signal oscillating at the frequency difference of the probes.

In this Letter, we describe the first observation of the temporal oscillation of an atomic wave packet localized in a periodic optical potential. When a potential is made to move very slowly by a small frequency difference, initially localized atoms will follow the moving potential and oscillate around the potential minimum. By detecting the transient response of the recoil-induced resonance, one can observe the temporal behavior of localized atomic motion.

In our experiment, a cold 4 μK cloud of ^{87}Rb atoms was produced [4] by a magneto-optical trap [7] and polarization-gradient cooling [8,9] in a rubidium-vapor cell. The $5S_{1/2}$, $F = 2$–$5P_{3/2}$, $F = 3$ cyclic transition of the ^{87}Rb D_2 line was used as a cooling cycle. After the preparation of the cold sample, two probe beams with wave vectors $\vec{k}_1, \vec{k}_2$ ($\vec{q} \equiv \vec{k}_2 - \vec{k}_1$) and angular frequencies ω_1, ω_2 ($\delta \equiv \omega_2 - \omega_1$) detuned from the atomic resonance by Δ, having parallel linear polarizations, are intersected inside the sample at an angle θ (Fig. 1). Because of the small frequency difference δ, an optical potential with a periodicity of $\cos(qr_q - \delta t)$, i.e., a potential moving with speed $v_0 = \delta/q$ along $\vec{q}$, was generated in the beam crossing area. Here $q = |\vec{q}|$, and r_q is the projection of the position vector on $\vec{q}$. The small fre-

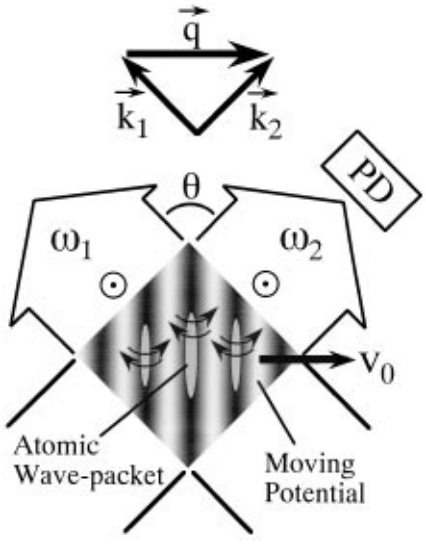

FIG. 1. An experimental scheme to observe the oscillation of an atomic wave packet localized in an optical potential. The optical standing wave moving with speed v_0 of δ/q is generated by two probe beams with wave vectors $\vec{k}_1$ and $\vec{k}_2$ and with angular frequencies ω_1, ω_2, which cross in the cold atomic vapor at an angle θ. Here $\delta = \omega_2 - \omega_1$, $\vec{q} = \vec{k}_2 - \vec{k}_1$, and $q = |\vec{q}|$. The intensity change of the transmitted probe beam is monitored by the photodetector (PD).

 0031-9007/96/76(14)/2428(4)$10.00

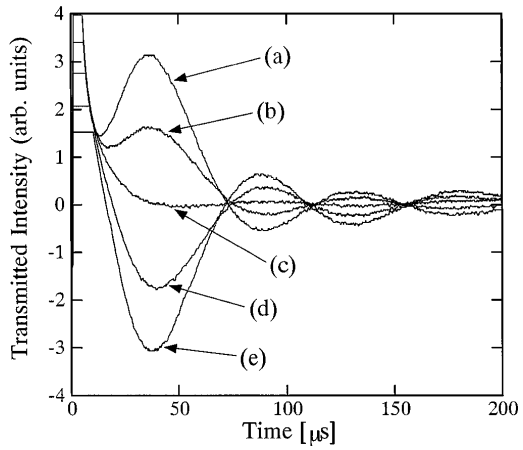

FIG. 2. Experimental results of the dependence of the transmitted intensity of the probe beam on frequency differences. Frequency differences $\delta/2\pi$ were (a) -8 kHz, (b) -4 kHz, (c) 0 kHz, (d) 4 kHz, and (e) 8 kHz, respectively.

quency difference between two probe beams was made by using acousto-optic modulators (AOM) [4]. We observed the transmitted intensity change of the probe beam as a signal by a photodetector.

In Fig. 2 we present typical transmitted probe signals. Here the intensity of the probe beams was 4 mW/cm^2, cross angle θ was 14.4°, and detuning was fixed at $\Delta/2\pi = -60$ MHz with respect to the $F = 2 - F = 3$ transition. The frequency difference $\delta/2\pi$ was set smaller than 8 kHz. Under these experimental conditions, the atomic kinetic energy in the frame of the moving optical potential $(m\delta/q)^2/2m \leq (4\hbar k)^2/2m$ was much smaller than the optical potential depth $(19\hbar k)^2/2m$. From this value, we can find that the signal oscillating frequency was independent of the value of $\delta/2\pi$ and the signal amplitude became larger as $\delta/2\pi$ increased from 0 kHz. Moreover, when the sign of $\delta/2\pi$ was reversed, the signal shape was also reversed.

We now describe the physical mechanism responsible for the signals observed here. As depicted in Ref. [4], the intensity change of the transmitted probe beam arises from the recoil-induced resonance [5,6] and can be represented by the imaginary part of the polarization P induced by two probe beams which is approximately given by

$$\mathrm{Im}\{P\} \cong -\frac{2\mu\Omega}{\Delta} \int dr_q \sin(qr_q - \delta t)\psi^*(r_q, t)\psi(r_q, t). \quad (1)$$

Here Ω, μ, and $\psi(r_q, t)$ are the Rabi frequency, the transition dipole moment, and the atomic wave function for center of mass motion. From Eq. (1), we can easily understand that the intensity change of the transmitted probe beam originates from a component of the atomic density distribution modulated by $\sin(qr_q - \delta t)$. Because the optical potential has a periodicity of $\cos(qr_q - \delta t)$, the time evolution of the atomic density distribution asymmetrical to the optical potential leads to a change in the transmitted probe intensity.

Next, we rewrite Eq. (1) with the vibrational eigenstates in the moving optical potential. We substituted the atomic wave function represented as a superposition of vibrational eigenstates, i.e., $\psi(r'_q, t) = \sum_n c_n \phi_n(r'_q) e^{-iE_n t/\hbar}$, into Eq. (1), where ϕ_n, c_n, and E_n are the eigenfunction, the probability amplitude, and the energy of the nth vibrational state, respectively, also $r'_q = r_q - \delta t/q$. By this substitution, Eq. (1) is rewritten as

$$\mathrm{Im}\{P\} \cong -\frac{2\mu\Omega}{\Delta} \sum_n \int dr'_q \sin(qr'_q) c_n^* c_{n+1} \phi_n^*(r'_q) \times \phi_{n+1}(r'_q) e^{-i(E_{n+1}-E_n)t/\hbar}. \quad (2)$$

From Eq. (2), we also observe that the quantum interference between even and odd numbered vibrational states leads to an intensity change of the probe beam. This is quite reasonable because such an interference makes the atomic density distribution asymmetrical with respect to the optical potential.

In our experiment, the initial atomic kinetic energy $(m\delta/q)^2/2m$ was much smaller than the potential depth. Therefore it is proper to interpret the damped oscillation in Fig. 2 as arising from the oscillation of an atomic wave packet localized in the potential due to the dynamic interference between the even and odd numbered vibrational states, as shown in Eq. (2).

In order to understand the dependence of the signals on the frequency difference shown in Fig. 2, we have simulated the time evolution of the atomic wave function inside a moving periodic optical potential and the corresponding recoil-induced resonance signal by using the Monte Carlo wave-function method [10]. In order to simulate the temporal behavior of an atomic wave packet, we have solved the master equation which consists of the relaxation operator and Hamiltonian given by Eqs. (67) and (77) of Ref. [10]. Evaluating Eq. (1), we have also obtained the transmitted intensity change of the probe beam. In this calculation, we treat atoms (here ^{87}Rb) as two-level atoms, and assume the initial atomic momentum distribution to be a δ function; i.e., the initial atomic density distribution is constant in all space. The cross angle, detuning, and Rabi frequency of each probe beam are assumed to be $\theta = 180°$, $\Delta = -\Gamma/2$, and $\Omega = \Gamma/2$, respectively, which give an optical potential depth of $(16\hbar k)^2/2m$. We set the moving speed of the optical potential v_0 such that $mv_0^2/2$ is much smaller than the potential depth. Note that since atoms oscillate in a one-dimensional optical potential, their characteristic behaviors can be observed for an arbitrary value of θ without any loss of generality. Therefore, for convenience, we have assumed a large value for θ, which decreases much of the computing time (as the angle increases, the reciprocal lattice vector of the optical potential increases, and thus the number of expansion coefficients of the atomic wave-function momentum space decreases, which then reduces the computing time).

Figures 3 and 4 present the numerical results of the time evolution of the atomic density distribution in the

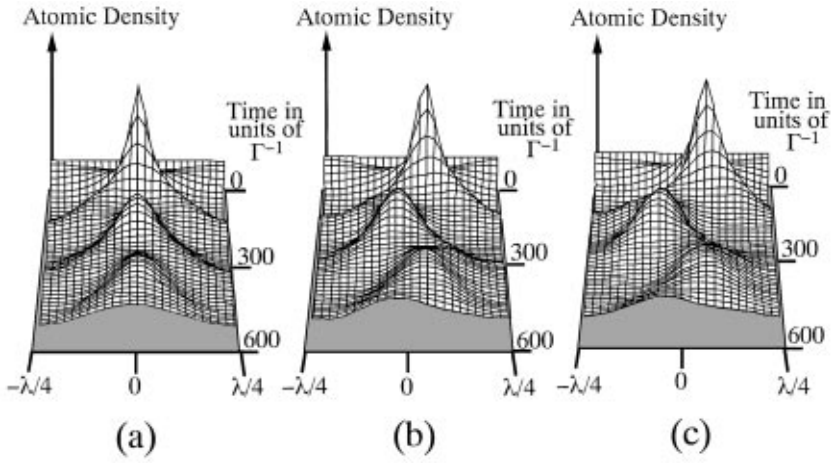

FIG. 3. The time evolution of the atomic density distribution in a periodic optical potential calculated by the Monte Carlo wave-function method. The detuning Δ and Rabi frequency Ω of each probe beam were $\Omega = -\Delta = \Gamma/2$, where the depth of the optical potential becomes $(16\hbar k)^2/2m$. The speeds of the optical potential v_0 were (a) 0, (b) $3\hbar k/m$, and (c) $5\hbar k/m$, respectively. The region of one period of an optical potential is considered, and the potential minimum is located at the origin on the spatial axis.

moving optical potential and the corresponding transmitted intensity change of the probe beam, respectively. Because the optical potential is spatially periodic, we show only the time evolution of the atomic density distribution inside one period of the optical potential in Fig. 3. The zero point on the spatial axis corresponds to the moving optical potential minimum.

In the case of a stationary optical potential, the spatially symmetrical vibrational states, i.e., even numbered (mainly 0th and 2nd) vibrational states, are excited because the initial atomic momentum is zero. Because of quantum interference between these even numbered vibrational states, the atomic density distribution oscillates symmetrically with respect to a potential with a frequency of $(E_2 - E_0)/\hbar$ (Bohr frequency) [Fig. 3(a)]. Because of the spatial symmetry of an atomic oscillation, the intensity of the probe beam does not change

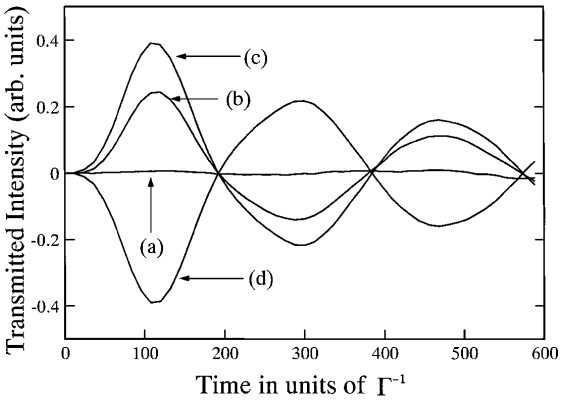

FIG. 4. The dependence of the transmitted intensity change on the moving speed of the optical potential v_0 calculated by the Monte Carlo wave-function method. The speeds of the potential v_0 were (a) 0, (b) $3\hbar k/m$, (c) $5\hbar k/m$, and (d) $-5\hbar k/m$, respectively. The detuning and Rabi frequency were the same as the values in Fig. 3.

[Fig. 4(a)]. Now, the reason why the signal amplitude became a minimum at $\delta/2\pi = 0$ kHz in Fig. 2 is clear; because at $\delta/2\pi = 0$ kHz, the optical potential is stationary.

In the case of a moving optical potential, spatially asymmetrical vibrational levels, i.e., odd numbered vibrational levels (mainly 1st), are also excited because the initial atomic momentum in the frame of the moving optical potential is nonzero. Because of quantum interference between even and odd numbered vibrational states, the atomic density distribution now oscillates asymmetrically with respect to the potential with a Bohr frequency of $(E_1 - E_0)/\hbar$ [Fig. 3(b)]. This additional atomic oscillation manifests itself as the damped oscillating signal [Fig. 4(b)]. As the moving speed of the optical potential increases, the population of odd numbered vibrational levels increases, and thus the amplitude of atomic oscillation, i.e., signal oscillation, increases [Figs. 3(c) and 4(c)]. When the moving direction of the potential is reversed, the time evolution of the atomic density distribution is also reversed spatially (we do not show this result in Fig. 3), and consequently the sign of the corresponding signal is reversed [Fig. 4(d)]. Here the reasons why the signal amplitude becomes larger as $\delta/2\pi$ is far from 0 kHz and why the signal shape is reversed when the sign of $\delta/2\pi$ is reversed in Fig. 2 are now clarified, because the moving speed of the optical potential is proportional to $\delta/2\pi$.

Moreover, in Fig. 4, the oscillation frequency of the signal is independent of the moving speed of the optical potential, which indicates that the oscillation frequency is determined only by the Bohr frequency between vibrational states. If the atoms traverse the optical potential, on the other hand, the signal oscillation frequency is determined by the time of flight for atoms traversing one period of the optical potential and thus strongly depends on the value of v_0 [4]. Therefore the fact that the oscillation frequency in Fig. 2 is independent of $\delta/2\pi$ is strong

evidence that we have observed localized atomic motion. Note that the Bohr frequencies can also be obtained by classical analysis, which implies that the oscillatory motion can be approximately understood as the classical harmonic oscillation.

As the simulation results show, the spatial localization of the atomic density distribution is gradually lost as time goes on [Figs. 3(a), 3(b), and 3(c)]. This is due to the fact that the quantum interference between atomic momentum states results in the spatial localization of the atomic density distribution. In other words, the atomic localization is gradually lost as spontaneous emission destroys the coherence between these momentum states. Such a dissipation of spatial localization of the atomic density distribution also manifests itself as the signal decay [Figs. 4(b), 4(c), and 4(d)]. Moreover, the signal decay time of $590\Gamma^{-1}$ representing the atomic coherence time is much longer than the inverse of the optical pumping rate Γ^{-1} at the antinodes of the optical standing wave. This can be explained by the fact that the energy separation between vibrational states is much larger than the recoil energy as a result of the strong confinement of the atomic wave function [11]. Similar effects appear in Fig. 2, where the signal decay time (40 μs) is much longer than the inverse of the optical pumping rate at the antinode of the optical standing wave (1 μs).

Note that the spatial localization of an atomic wave packet can also be lost due to the dephasing effect between different vibrational states. Moreover, the atomic wave packet is repeatedly squeezed and stretched during the asymmetrical oscillatory motion [Figs. 3(b) and 3(c)]. This indicates that the atomic wave function which is not in a coherent state is equivalent to a classical harmonic oscillator. Therefore, quantum mechanical treatments may be needed for fully understanding these effects.

Finally, we have checked that the signals observed here originate from the localized atomic motion by using another method. We compared the signal oscillation frequency and the theoretically calculated Bohr frequency $\Delta\omega_{\mathrm{vib}} = (E_1 - E_0)/\hbar$ under various depths of the optical potential, i.e., various detunings of probe beams. The intensity and the cross angle of the probe beams were set equal to the values in Fig. 2. The frequency difference $\delta/2\pi$ was fixed at 4 kHz. In Fig. 5, dots represent the experimental data and the solid curve represents the theoretically calculated Bohr frequency $\Delta\omega_{\mathrm{vib}}$. We also show a comparison between experimental oscillating frequencies and the theoretically calculated Bohr frequencies in the inset of Fig. 5. The slope of the fitted line is 0.9, which is smaller than unity. This slight systematic deviation can be attributed to the imperfect contrast of the interference between the probe beams whose wave fronts are not, in practice, perfectly plane. The slightly distorted wave fronts reduce the effective optical potential depth so that the experimental values become slightly smaller than the ideal theoretical values.

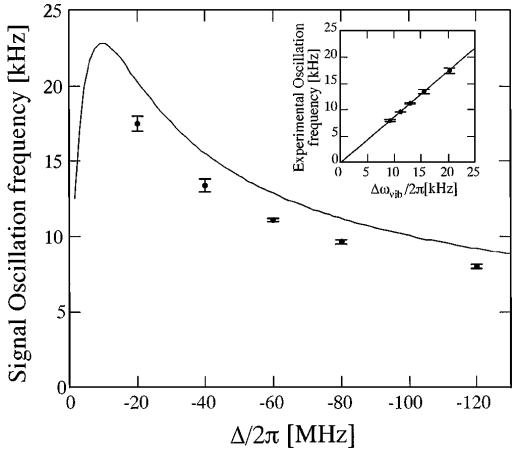

FIG. 5. The dependence of the signal oscillating frequency on probe detuning $\Delta/2\pi$. The intensity and cross angle of the probe beams were equal to the values in Fig. 2. The frequency difference $\delta/2\pi$ was fixed at 4 kHz. Dots represent the experimental results, and the solid curve represents the theoretical Bohr frequencies $\Delta\omega_{\mathrm{vib}}/2\pi$ between 0th and 1st vibrational states. Inset shows the comparison between experimental oscillating frequencies and theoretical Bohr frequencies. The slope of the fitted line was 0.9.

In summary, we have demonstrated the novel *in situ* method to observe the oscillating motion of an atomic wave packet localized in a periodic optical potential. Our method will be a powerful tool for investigating the fundamental dynamics of cold atoms localized in an optical potential.

The authors wish to thank Dr. A. Hemmerrich (University of Munich) and Dr. W. D. Phillips (NIST) for their valuable comments and discussions.

[1] P. Verkerk, B. Lounis, C. Salomon, C. Cohen-Tannoudji, J.-Y. Courtois, and G. Grynberg, Phys. Rev. Lett. **68**, 3861 (1992).
[2] C. I. Westbrook, R. N. Watts, C. E. Tanner, S. L. Rolston, W. D. Phillips, P. D. Lett, and P. L. Gould, Phys. Rev. Lett. **65**, 33 (1990).
[3] P. S. Jessen, C. Gerz, P. D. Lett, W. D. Phillips, S. L. Rolston, R. J. C. Spreeuw, and C. I. Westbrook, Phys. Rev. Lett. **69**, 49 (1992).
[4] M. Kozuma, Y. Imai, K. Nakagawa, and M. Ohtsu, Phys. Rev. A. **52**, R3421 (1995).
[5] D. R. Meacher, D. Boiron, H. Metcalf, C. Solomon, and G. Grynberg, Phys. Rev. A **50**, R1992 (1994).
[6] J. Guo, Phys. Rev. A **49**, 3934 (1994).
[7] E. L. Raab, M. Prentiss, Alex Cable, Steven Chu, and D. E. Pritchard, Phys. Rev. Lett. **59**, 2631 (1987).
[8] C. Salomon, J. Dalibard, W. D. Phillips, A. Clairon, and S. Guellati, Europhys. Lett. **12**, 683 (1990).
[9] C. Monroe, W. Swann, H. Robinson, and C. Wieman, Phys. Rev. Lett. **65**, 1571 (1990).
[10] K. Mølmer, Y. Castin, and J. Daribard, J. Opt. Soc. Am. B **10**, 524 (1993).
[11] J. Courtois and G. Grynberg, Phys. Rev. A **46**, 7060 (1992).